Geologica Acta, Vol. 13, Nº 3, September 2015, 211-228
DOI: 10.1344/GeologicaActa2015.13.3.4

The Pliocene Mediterranean infilling of the Messinian Erosional Surface: New biostratigraphic data based on calcareous nannofossils (Bajo Segura Basin, SE Spain)

C. LANCIS[1] J.E. TENT-MANCLÚS[1*] J.A. FLORES[2] J.M. SORIA[1]

[1]Departamento de Ciencias de la Tierra y del Medio Ambiente, Universidad de Alicante
Apto. 99. 03080 San Vicente del Raspeig. Alicante, Spain. Lancis E-mail: Carlos.lancis@ua.es, Tent-Manclús E-mail: je.tent@ua.es, Soria E-mail: jesus.soria@ua.es Fax: (+ 34) 965909862

[2]Departamento de Geología, Universidad de Salamanca
Plaza de la Merced s/n, 37008-Salamanca, Spain. E-mail: flores@usal.es Fax: (+ 34) 923294514

*Corresponding author

ABSTRACT

The Bajo Segura Basin (eastern Betic Cordillera) is a Mediterranean marginal basin where the Messinian Erosional Surface (MES), formed during the Messinian Salinity Crisis sea-level fall, is well developed. Overlying this major discontinuity the lower Pliocene transgressive sediments record the reflooding of the Mediterranean and the return to an open marine environment, the continental shelf being rebuilt after the Messinian erosion. The stratigraphic and biostratigraphic study of six sections allows two transgressive-regressive sequences filling the MES to be distinguished, correlated with the previously distinguished Mediterranean offshore seismic units. Ten calcareous nannofossil bioevents have been identified. The lower sequence can be dated according to nannofossil biozones NN12 to NN14 and the upper sequence by NN15 to NN16. The boundary between both lower Pliocene sedimentary sequences occur after the first common occurrence (FCO) of *Discoaster asymmetricus* found in the uppermost sediments of the lower sequence and before the first occurrence (FO) of *Discoaster tamalis* in the lowermost part of the upper sequence. Thus this sequence boundary can be estimated at between 4.1 and 4.0Ma ago.

KEYWORDS **Pliocene. Messinian Erosional Surface. Messinian Salinity Crisis. Zanclean. Calcareous nannofossils.**

INTRODUCTION

The Messinian Erosional Surface (MES, Cita and Ryan, 1978) is a subaerial erosional surface that deeply cuts the continental margins and developed during the acme of the Messinian Salinity Crisis (MSC, Ryan *et al*., 1973), when the Mediterranean sea-level dropped more than 1000 meters and shallow-water evaporite precipitation was shifted to the deepest parts (Roveri *et al*., 2006). The rise in global sea level at the beginning of the Early Pliocene (Haq *et al*., 1987), probably combined with a change in the tectonic activity in the Alboran Sea area, caused the flooding of the desiccated basin (Zanclean transgression). This rise in sea level marked the end of the salinity crisis with the re-establishment of open marine conditions in the Mediterranean. From that time onward, the Early Pliocene was marked by a long period (about 1.7Ma) of high sea level in which the Mediterranean margins were re-built by the sedimentary infill of the MES (Clauzon *et al*., 1987). Many recent works (Rabineau, 2001; Lofi *et al*., 2003; 2005; 2011; Duvail *et al*., 2005; Bache, 2008; Bache *et al*., 2009; 2010; 2012; García *et al*., 2011; Urgeles *et al*., 2011; Maillard *et al*., 2011; Leroux, 2013) have described and quantified the Pliocene–Quaternary Mediterranean sedimentation,

based on a broad database of seismic reflection profiles. The prograding sedimentary prisms migrated rapidly seaward and filled the underlying Messinian topographic lows. This contribution aims to improve our understanding of the Early Pliocene transgression and the re-building of the Mediterranean continental margin after the major Messinian erosion of the Miocene continental shelves by studying the stratigraphy and nannofossil assemblages of onshore well-exposed Lower Pliocene sediments.

GEOLOGICAL SETTING

The Betic Cordillera, located in the southeast of the Iberian Peninsula, has an ENE–WSW trend and has classically been divided into two major zones (Fig. 1): the External Zone, adjacent to the Iberian foreland and mainly composed of sedimentary rocks, and the Internal Zone, farther away from the foreland and composed mainly of metamorphic rocks (Fallot, 1948). Before the MSC occurred, two straits, the Northbetic and the Rifian, both representing the foreland of the Betic and Rif cordilleras, formed the Atlantic-Mediterranean passages. The building up of the Betic and Rif cordilleras produced a narrowing and partial closure of the passages (Viseras *et al*., 2004). The onset of the MSC was a consequence of this seaway restriction, and the opening of the Strait of Gibraltar marked the end of the MSC (Ryan *et al*., 1973).

Previous works carried out in the Bajo Segura Basin, a Mediterranean marginal Betic basin with evaporite deposits during the MSC (Caracuel *et al*., 2004; 2011; Soria *et al*., 2005; 2008a, b; García-García *et al*., 2011; Martínez del Olmo, 2011a), have described a major erosional surface separating the Upper Messinian deposits, mostly non-marine, and the overlying Pliocene marine transgressive deposits. The most significant features of this surface, assigned to the MES are broad paleovalleys up to 200m deep (Caracuel *et al*., 2004; 2011; Soria *et al*., 2008a; 2008b; García-García *et al*., 2011; Martínez del Olmo, 2011a).

Recent studies of the MES in seismic profiles (Bache, 2008; Bache *et al*., 2009; García *et al*., 2011; Martínez del Olmo 2011b; Bache *et al*., 2012) have differentiated "rough or badland" morphology and a more basinward "smooth" surface. The latter deepens slightly seaward and extends over 60–70km (Bache *et al*., 2009). The transition between the two morphologies (rough and smooth) is very clear and lies at a constant two-way-traveltime depth of 1.6 seconds over most of the Provence shelf (Bache, 2008; Bache *et al*., 2009) and the Valencia trough (Martínez del Olmo, 2011b). Bache *et al*. (2012) interpreted this surface as the result of a two-step process for the reflooding of the Mediterranean after the MSC, suggesting an initial moderate and relatively slow reflooding accompanied by transgressive ravinement, followed by a second very rapid step that preserved the subaerial MES. The amplitude of these two successive rises in sea level were estimated by Bache *et al*. (2012) at ≤500m for the first rise and 600–900m for the second rise. According to these authors the start of the second step preceded the Zanclean Global Stratotype Section and Point in Eraclea Minoa (Sicily, Van Couvering *et al*., 2000; Hilgen *et al*., 2012), and therefore starts before the end of the Messinian (Bache *et al*., 2012). The Bajo Segura Basin sections studied here may correspond to the latest Messinian-earliest Pliocene sediments filling the "rough" MES topography.

THE TRANSGRESSIVE PLIOCENE

Six stratigraphic sections have been studied (Fig. 2). The Pedrera section (PE), previously studied by Lancis *et al*. (2004a) and Soria *et al*. (2008a), is located to the west of the La Pedrera dam. The Pantano de Elche section (PTEL) outcrops in the eastern margin of the Vinalopó river cut (just below the A7-highway bridge to the north of the city of Elche). The Guardamar de Segura section (GUA) is found to the west of the village of the same name; the bottom of the section is at the north of the cemetery and runs following an access road to the water deposit of the village. The San Miguel de Salinas (SM) is the "Canal del Transvase Tajo Segura" section (a water channel) located to the west of the town of San Miguel de Salinas, previously studied by Corbí Sevila (2010). The beds dip 10º to 20º to the east. The Dehesa de Pino Hermoso section (DPH) is located to the southwest of the village of Arneva. As the section bedding tilts to the west it runs across different orange groves in the same direction. The Santa Pola section (SP) corresponds to the northern side of the Santa Pola Sierra, in the Clot de Galvany protected forest area (previously studied by Lancis *et al*., 2004b). The section runs along the southern side of the "Cabeço" hill, just west of the La Charca lagoon.

Current knowledge of the Early Pliocene transgression of the Eastern Betic Cordillera basins is based on the work by Montenat (1977), and a later synthesis by Montenat *et al*. (1990). The uppermost Messinian sedimentation mainly occurred in continental environments (Montenat, 1977; Montenat *et al*., 1990; Soria *et al*., 2005; 2008a; 2008b; Caracuel *et al*., 2011), eroded by incised paleo-valleys, filled by high-energy sediments (Caracuel *et al*., 2004; 2011; García-García *et al*., 2011), and covered by open marine, white marls (Soria *et al*., 1996; 2008a; 2008b). These white marls belong to an Early Pliocene major allostratigraphic unit (P unit, according to Caracuel *et al*., 2006), which forms a shallowing-upward sequence composed of four main terms (Caracuel *et al*., 2006): i)

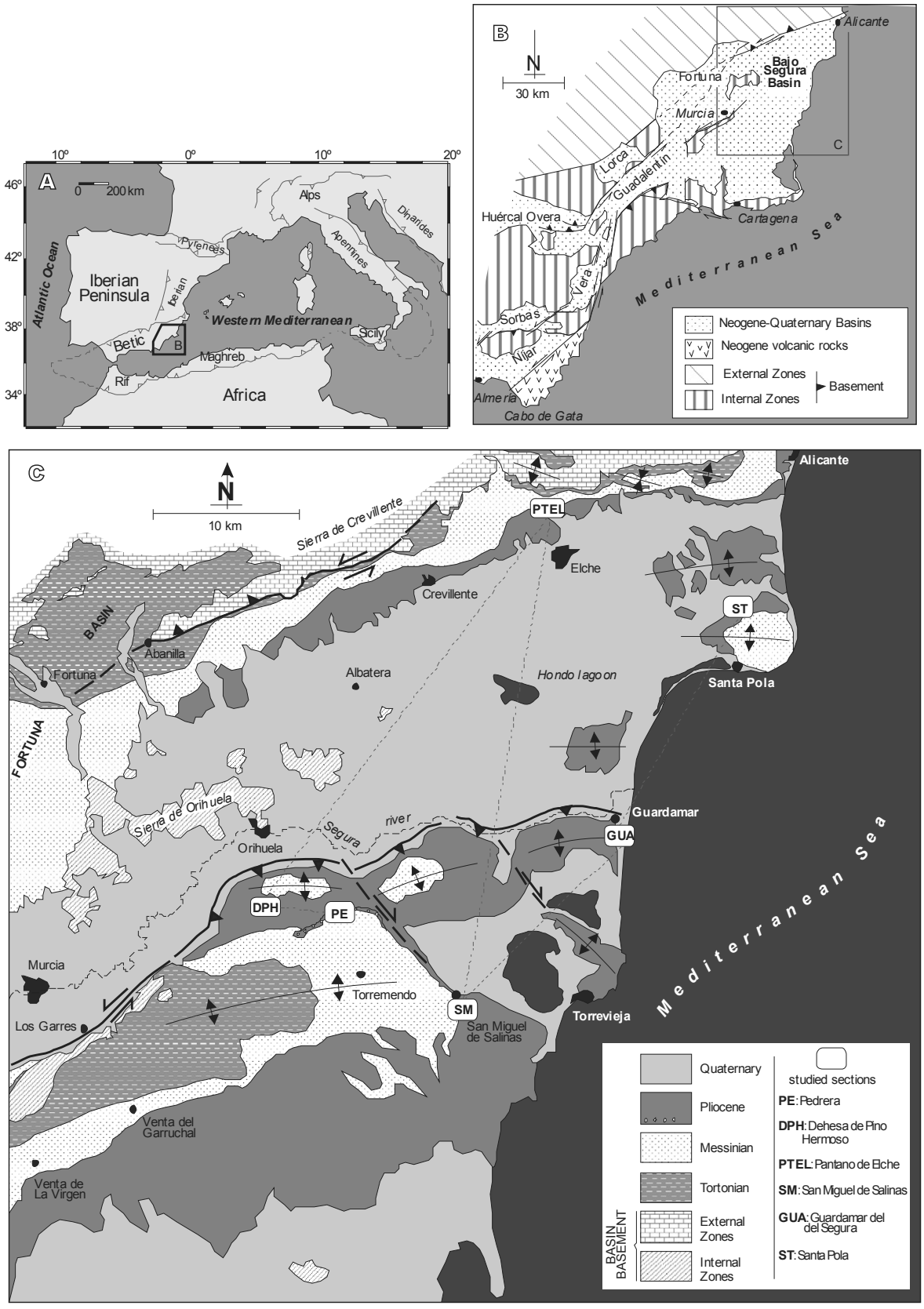

FIGURE 1. A) Location of the Betic Cordillera in the western Mediterranean. B) Geological map of the eastern end of the Betic Cordillera showing the position of the Bajo Segura Basin. C) Geological map of the Bajo Segura Basin (simplified from Montenat, 1990). The dashed line marks the correlation chart in Figure 2.

the basal high-energy lag, or P0, of the Early Pliocene transgression, and the high-energy paleo-valley fills (Pedrera formation in Soria *et al.*, 2008a); ii) the lower white "Hurchillo marls", P1 in Montenat *et al.* (1990); iii) the middle yellow calcareous sandstone, "Rojales sandstone" or P2 (Montenat *et al.*, 1990), interpreted as transitional environments from shoreface to foreshore and ending with backshore and aeolian sand dunes (Soria *et al.*, 2005), and iv) the upper continental "variegated sands and marls", and the laterally lacustrine equivalent San Pedro

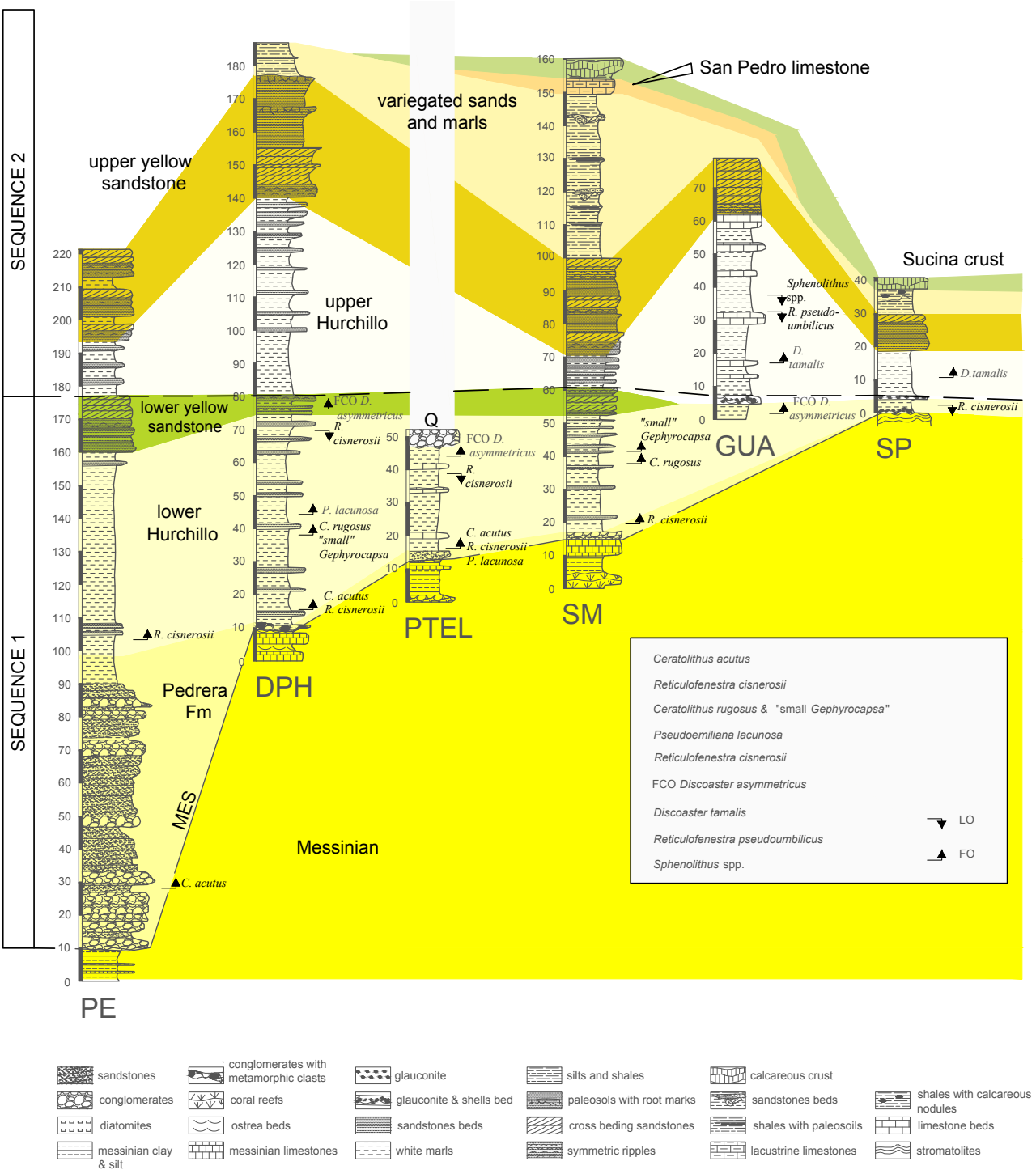

FIGURE 2. Stratigraphic sections of the lower Pliocene sediments in the Bajo Segura Basin. Sections PE: Embalse de la Pedrera; DPH: Dehesa de Pino Hermoso; PTEL: Pantano de Elche; SM: San Miguel de Salinas; GUA: Guardamar de Segura; SP: Santa Pola; Q: Quaternary; FO: First Occurrence; LO: Last Occurrence; FCO: First Common Occurrence.

limestone, both included in P3 (Montenat *et al.*, 1990). The paleo-valley fill and the overlying Hurchillo white marls of the Bajo Segura Basin can be the result of the second transgressive step of Bache *et al.* (2012), and may be interpreted as just the bottom part of the latest Messinian-earliest Pliocene sediments covering the MES

.

The classic scheme of the Bajo Segura Basin based on P0, P1, P2 and P3 (see Soria *et al.*, 2005) can be updated. There are white Hurchillo marls above and below the yellow calcareous sandstone in the PE and DPH sections (Fig. 2). Both levels of white marl have the same facies but different nannofossil contents, allowing them to be separated as the lower Hurchillo marls and the upper Hurchillo marls. The latter has an upper yellow calcareous sandstone showing the same transitional facies, ending with aeolian sand dunes, that the lower yellow sandstone. The two yellow calcareous sandstones show several shallowing-upward sequences like the ones described by Soria *et al.* (2005) for the P2, that is, from bottom to the top: i) sands with bivalves (ostreids and pectinids) and abundant traces of *Thalassinoides*, in the upper part of which sets of cross stratification caused by the migration of sand waves occur; ii) sands and gravels with bivalves and conglomerates bored by *Lithophaga*, and iii) well-sorted sands, without fossils, with high-angle cross stratification formed by the migration of aeolian dunes, in which levels of stromatolites and thin channels of gravels are intercalated.

Two shallowing sequences seem to develop in the lower yellow calcareous sandstone (PE, DPH, and SM; Fig. 2). However the more basinward sections (GUA and SP) do not record the lower yellow calcareous sandstone. Instead, the lower and upper Hurchillo marls are separated in the GUA section by a glauconitic level, with abundant bivalve shells and fish teeth. In the SP section the lower Hurchillo marls is glauconitic-rich and the limit between the lower and upper Hurchillo is a coquina of brachiopod shells (Lancis *et al.*, 2004b). The most basinward SP section is found to the north of the Santa Pola Messinian reef (Calvet *et al.*, 1996; Feldman and McKenzie, 1997), a palaeohigh of the MES, that may cause the starvation of the SP section and the formation of glauconite.

The upper yellow calcareous sandstone shows 3 sequences in PE, SM, and DPH (lower sequence well developed, followed by 2 massive sand levels capped by paleosols with root marks, Fig. 2) and 1 in the more distal GUA and SP sections.

The new scheme of for the Bajo Segura Basin Pliocene can be inferred from the Figure 2. A lower sequence formed by: a basal lag and the Pedrera Formation, covered by the lower Hurchillo marls and then capped by the lower yellow sandstone. While the upper sequence is made by the upper Hurchillo marls capped by the upper yellow sandstone, and then overlaid by the variegated sands and marls and the San Pedro limestone. The lower sequence in the studied sections have neither variegated sands and marls nor the San Pedro lacustrine limestone.

METHODS

All sections were sampled by Lancis (1998) to study their nannofossil assemblages quantitatively, except the SP section, studied qualitatively in Lancis *et al.* (2004b). Twenty-five samples were collected from the PE section, 10 from the SM section, 26 from the PTEL section, 23 from the GUA section, 33 from DPH (Lancis, 1998), and 8 from the SP section (Lancis *et al.*, 2004b). For each sample collected, four different smear slides were prepared, using a method aimed at increasing the nannofossil-to-silt ratio (Lancis, 1998). For the first smear slide, 0.1g of sediment was suspended in 10ml distilled water (buffered at pH 8) spread on a 300mm^2 surface in one case (direct suspension, without dilution) and in the other smear slide after a 1/3 dilution of the suspension with distilled water (buffered at pH 8). In order to increase smear slide quality, a second procedure was performed as follows. A 10ml suspension of 0.1g sediment in distilled water (buffered at pH 8) was centrifuged at 1800rpm (450g) for 2 minutes at room temperature. After discarding the supernatant, distilled water was added to the pellet to achieve a 10ml suspension and the new mixture was subjected to sonication for 8 seconds. This centrifugation-sonication procedure was repeated five times. Finally, 0.1ml of the suspension was extended directly, covering a 300mm^2 over the surface of the slide, without dilution for the third smear slide and after 1/3 dilution with distilled water (buffered at pH 8) for the fourth one. The four prepared smear slides of each sample were analysed quantitatively under a 100x objective, scanning the whole slide to detect rare biostratigraphic markers. The percentage of nannoliths >3μm was determined after counting 500 nannoliths larger than 3μm. For counting "small reticulofenestrids" (<3μm), the mean values were calculated using the percentage of those coccoliths found in 10 visual fields, counting around 3000 nannoliths. Finally, the percentages of the different species of *Discoaster* spp. were calculated, counting 100 asteroliths.

BIOSTRATIGRAPHY

The biozonal schemes of Martini (1971) and Okada and Bukry (1980) were adopted for the Pliocene interval in the sections studied. In addition, other bioevents were used to improve nannofossil biostratigraphy based on Driever (1988), Fornaciari *et al.* (1990, 1996), Rio *et al.* (1990),

Bukry (1992), Young *et al.* (1994), Raffi and Flores (1995), Lancis (1998), Marino and Flores (2002), Lancis and Flores (2006), Lourens *et al.* (2004), and Raffi *et al.* (2006). Martini's (1971) Zones NN14 and NN15 were combined by Rio *et al.* (1990a) because of the rarity of the Zone NN14/NN15 boundary bioevent, the last occurrence (LO) of *Amaurolithus tricorniculatus*, in the Mediterranean region. Figure 3 shows the correlation chart based on the scheme by Lourens *et al.* (2004) and the chronostratigraphy by Hilgen *et al.* (2012). Our biostratigraphic analysis yielded a number of calcareous nannofossil events that appeared to be useful to improve the biostratigraphic resolution of the Early Pliocene.

Calcareous nannofossil assemblages

The nannofossil assemblage of the lower Hurchillo marls is characterized by an abundance of *Reticulofenestra cisnerosii* (Lancis and Flores, 2006) together with the presence of scarce *Ceratolithus acutus* in the bottom samples (Figs. 4; 5). The most abundant group is the "small reticulofenestrids", although the species *Coccolithus pelagicus, Reticulofenestra pseudoumbilicus* >7μm, *Reticulofenestra haqii/minutula, Sphenolithus abies, Sphenolithus neoabies, Scyphosphaera lagena, Helicosphaera carteri, Helicosphaera selli, Calcidiscus macintyrei, Calcidiscus leptoporus, Umbilicosphaera rotula, U. jafari,* and *Dictycoccites antarcticus* are also abundant. The "small Gephyrocapsa spp.", and *Pseudoemiliania lacunosa* (Figs. 6; 7; 8; 9; 10; 11) appear in the upper part of the studied interval.

Asteroliths are frequent, especially *Discoaster pentaradiatus, D. asymmetricus,* and *D. brouweri*, while *D. surculus, D. quinqueramus,* and *D. berggreni* are absent (Figs. 6; 7; 8; 9; 10; 11).

The top part of the sections shows the first occurrence (FO) of *Discoaster tamalis* and the disappearance of *Reticulofenestra pseudoumbilicus*, and *Sphenolithus* spp.

Calcareous nannofossil events and biochronology

In our sections, ten calcareous nannofossil biovents can be recognized from bottom to top (Figs. 3; 4; 5): i) the FO of *Ceratolithus acutus*, ii) the FO of *Reticulofenestra cisnerosii*, iii) the FO of *Ceratolithus rugosus*, iv) the FO of "small Gephyrocapsa spp.", v) the FO of *Pseudoemiliana lacunosa*, vi) the LO of *Reticulofenestra cisnerosii*, vii) the first common occurrence (FCO) of *Discoaster asymmetricus*, viii) the FO of *Discoaster tamalis*, ix) the LO of *Reticulofenestra pseudoumbilicus*, and x) the LO of *Sphenolithus* spp.

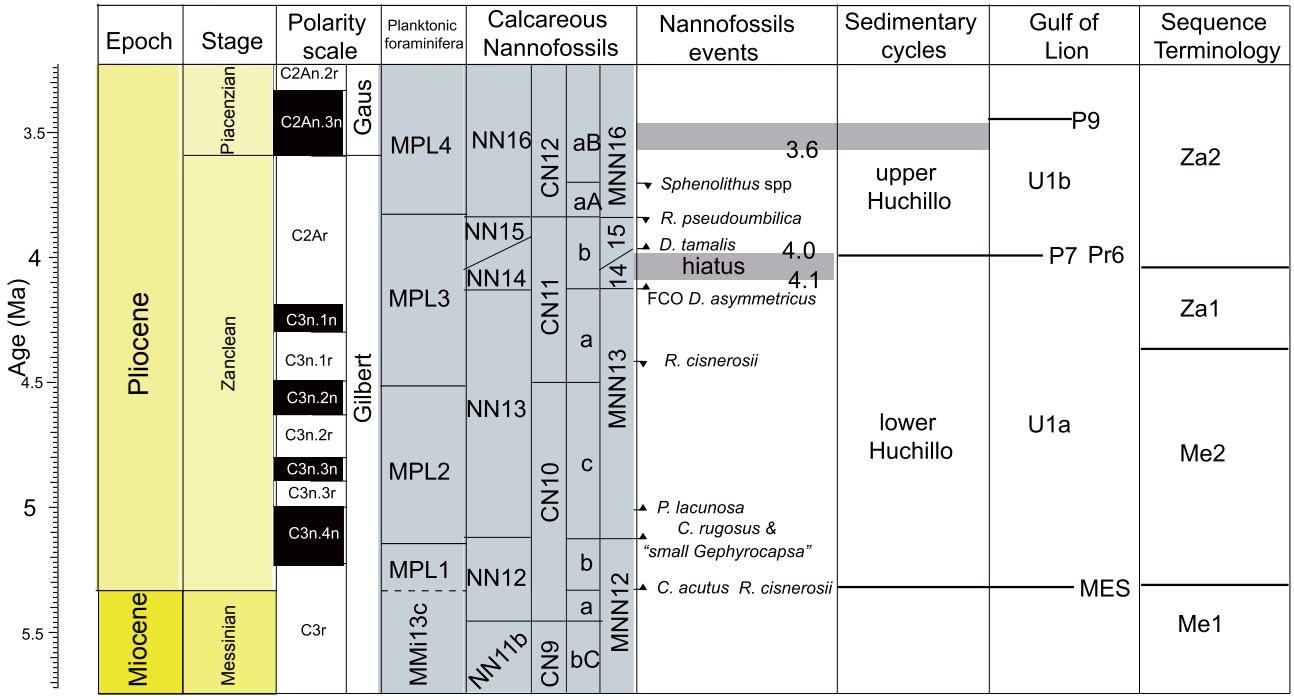

FIGURE 3. Calcareous nannofossil events in the Bajo Segura Basin. The planktonic foraminifera scale is the Mediterranean eastern scale from Lourens *et al.* (2004). The NN zonation is from Martini (1971); the CN zonation is from Bukry (1975) and the emended CN is from Okada and Bukry (1980) and Bukry (1991), and the MNN is from Rio *et al.* (1990). Correlation between the different scales is based in Lourens *et al.* (2004). The Gulf of Lion column shows the reflectors Pr6 from Duvail *et al.* (2005); p7 and p9 from Rabineau (2001), and the seismic units: U1-a and U1-b from Lofi *et al.* (2003). The sequence terminology is based on Snedden and Liu (2011). Cronostratigraphy by Hilgen *et al.* (2012).

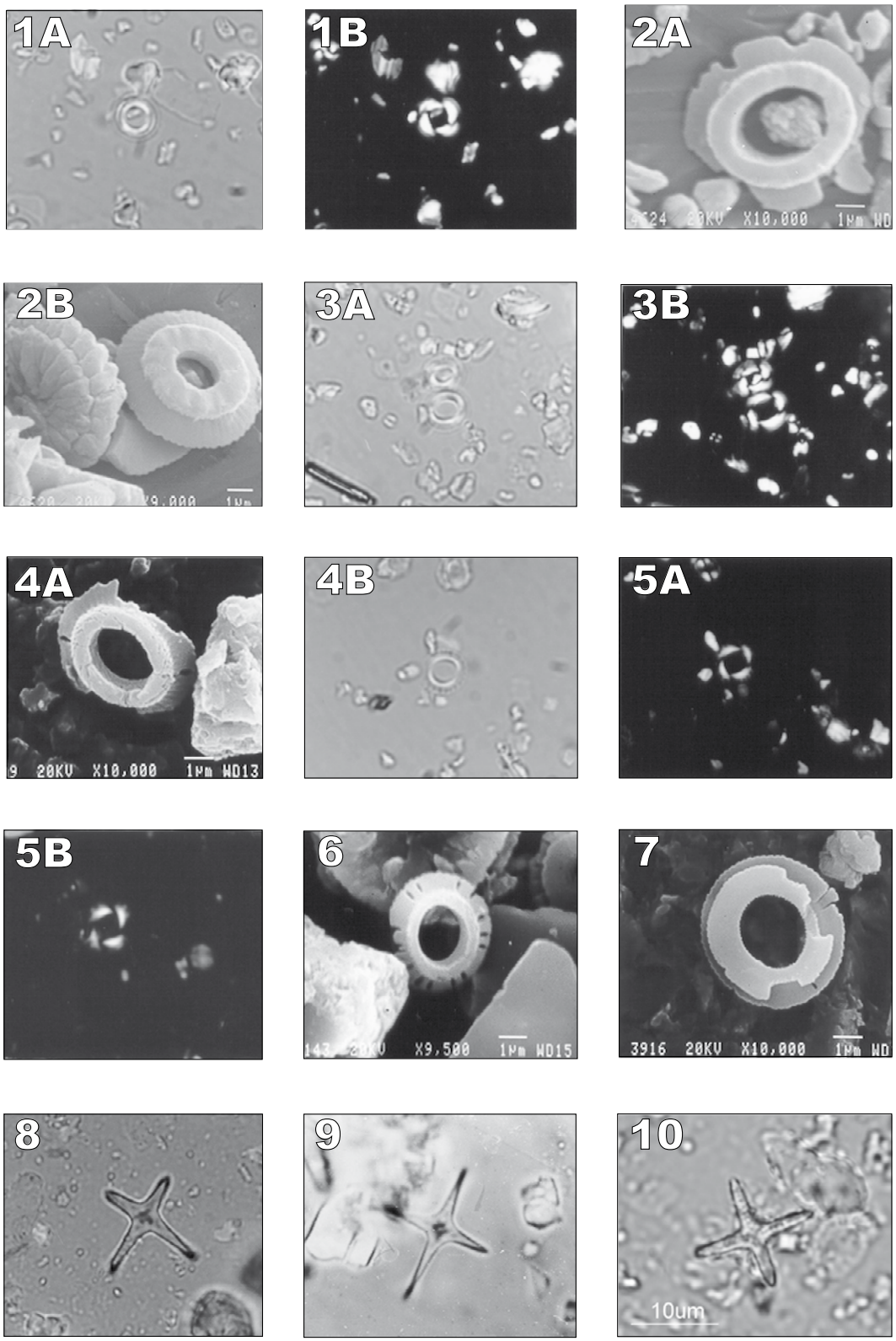

FIGURE 4. 1A) *Reticulofenestra cisnerosii* 1500x sample DPH-20, plane light; 1B) *Reticulofenestra cisnerosii* 1500x sample DPH-20, crossed polars; 2A) *Reticulofenestra cisnerosii* sample PTEL-6, Scaning Electronic Microscope (SEM); 2B) *Reticulofenestra cisnerosii* sample PTEL-6, SEM; 3A) *Reticulofenestra cisnerosii* 1500x sample DPH-14, plane light; 3B) *Reticulofenestra cisnerosii* 1500x sample DPH-14, crossed polars; 4A) *Pseudoemiliana lacunosa* sample GUA-1, SEM; 4B) *Pseudoemiliana lacunosa* 1500x sample GUA-20, Parallel plane light; 5A) *Pseudoemiliana lacunosa* 1500x sample GUA-20, Crossed polars; 5B) *Pseudoemiliana lacunosa* 1500x sample GUA3, Crossed polars; 6) *Pseudoemliana lacunosa* sample GUA-1 SEM; 7) *Pseudoemiliana lacunosa* sample GUA-1 SEM; 8) *Discoaster tamalis* 1500x sample GUA-16, plane light; 9) *Discoaster tamalis* 1500x sample GUA-14, plane light; 10) *Discoaster tamalis* 1500x sample SP-3, plane light.

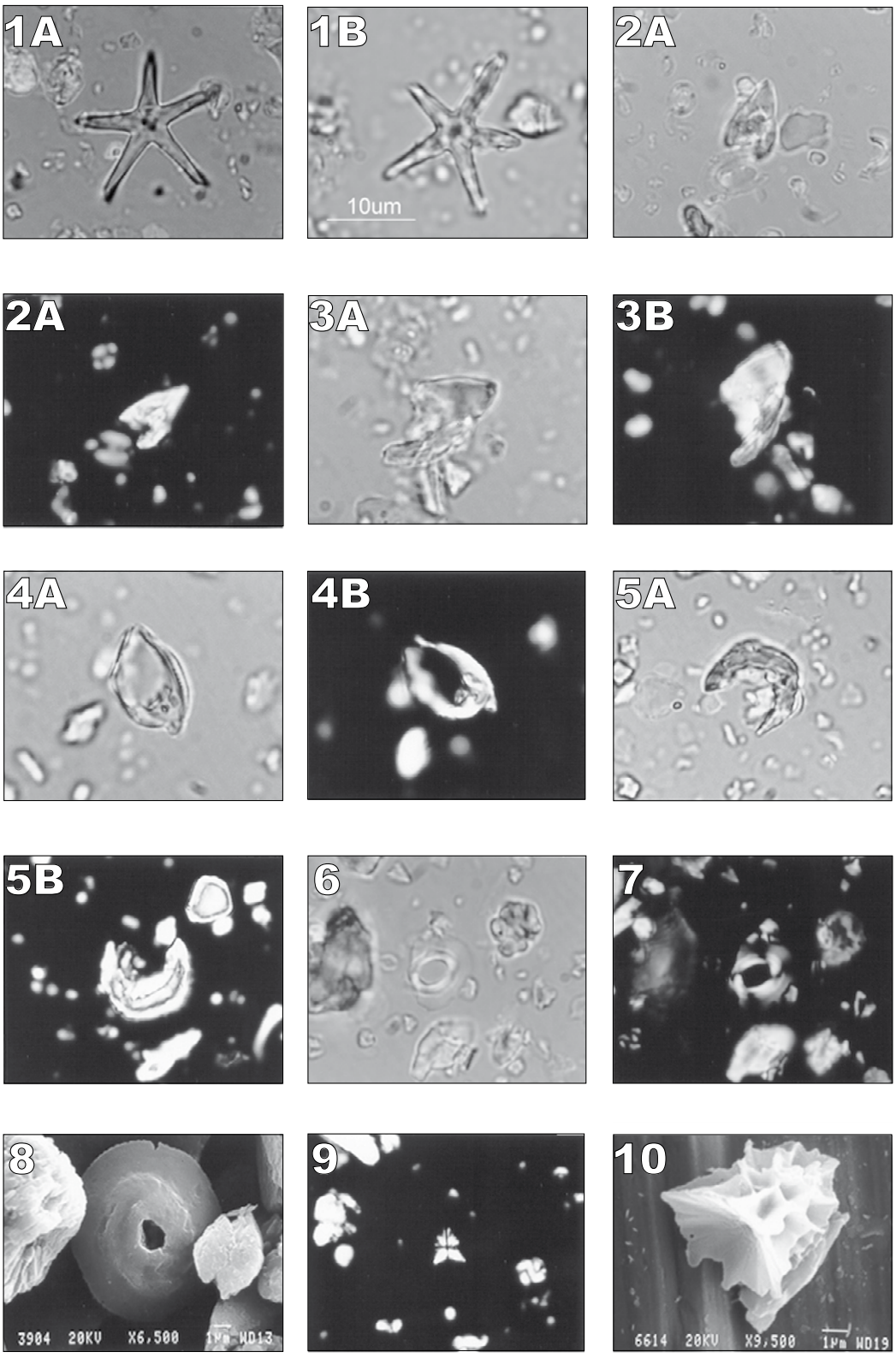

FIGURE 5. 1A) *Discoaster asymmetricus* 1500x sample GUA-16, plane light; 1B) *Discoaster asymmetricus* 1500x sample SPL-5, plane light; 2A) *Ceratolithus acutus* 1500x sample PTEL-6, plane light; 2B) *Ceratolithus acutus* 1500x sample PTEL-6, Crossed polars; 3A) *Ceratolithus acutus* 1500x sample GUA-1, plane light; 3B) *Ceratolithus acutus* 1500x sample GUA-1, Crossed polars; 4A) *Ceratolithus armatus* 1500x sample DPH-13, plane light; 4B) *Ceratolithus armatus* 1500x sample DPH-13, Crossed polars; 5A) *Ceratolithus rugosus* 1500x sample DPH-14, plane light; 5B) *Ceratolithus rugosos* 1500x sample DPH-14, Crossed polars; 6) *Reticulofenestra pseudoumbilicus* 1500x sample DPH-20, plane light; 7) *Reticulofenestra pseudoumbilicus* 1500x simple DPH-20 Crossed polars; 8) *Reticulofenetra pseudoumbilicus* sample GUA-1, SEM; 9) *Sphenolithus abies* 1500x sample DPH-13, Crossed polars; 10) *Sphenolithus abies* sample PE-148, SEM.

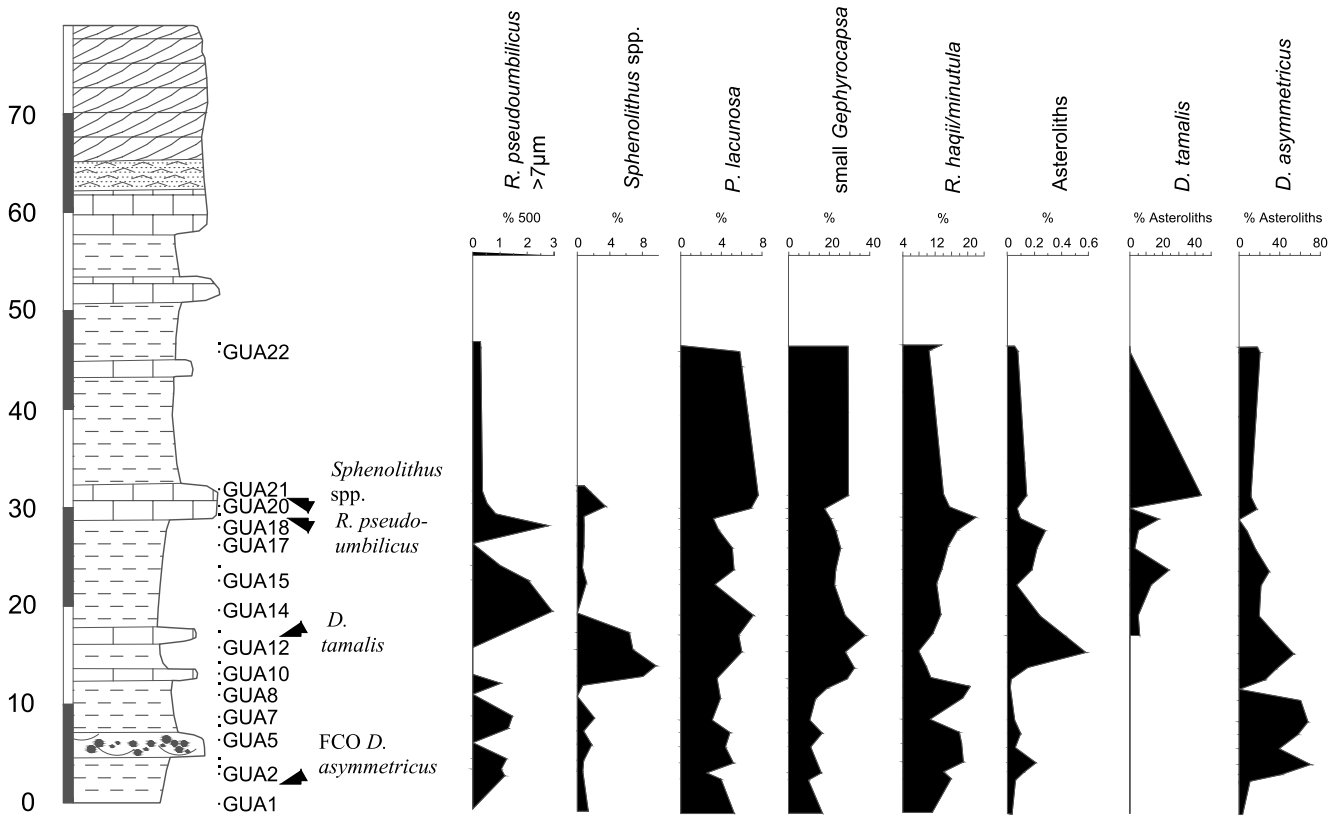

FIGURE 6. Quantitative distribution patterns of selected nannofossils in the Guardamar de Segura (GUA) section. Percentages are relative to 500 specimens >3µm counted (500%). The percentage of "small *Gephyrocapsa*" is calculated relative to all the nanoliths (%). The *Discoaster tamalis* and *Discoaster asymmetricus* percentage is calculated relative to all the asteroliths (asteroliths %). See section Methods. Note differences in scaling.

The FO of *Ceratolitus acutus* marks the CN10a/CN10b Boundary (Okada and Bukry, 1980), and has been considered as the standard event indicating the Messinian/Pliocene (M/P) boundary (Lourens *et al.*, 2004). Shackleton and Crowhurst (1997), and Backman and Raffi (1997) proposed an age of 5.35Ma for *C. acutus* FO in the equatorial Atlantic. In the Mediterranean, the FO of *C. acutus* was delayed until the beginning of the Pliocene (Cita and Gartner, 1973; Castradori, 1998; Van Couvering *et al.*, 2000) because of the isolation of the basin during the MSC. In the Mediterranean, recordings of the FO of *C. acutus* are rare. Sometimes broken and overgrowth *Amaurolithus primus* (showing birefringence) may be mistaken for *C. acutus*. Lancis (1998) uses these overgrowth *Amaurolithus* forms to mark the uppermost marine Messinian. *C. acutus* has been found sporadically in the PE, DPH, and PTEL sections.

The FO of the abundant *Reticulofenestra cisnerosii* has been proposed by Lancis (1998), and Lancis and Flores (2006) as an alternative event to the FO of *C. acutus* for the M/P boundary in the Mediterranean basins. Although the FO of *R. cisnerosii* was initially identified in chron C3n.4n, Soria *et al.* (2008a) in a later study recalibrated this event as C3r in the PE section. Also, Di Stefano and Sturiale (2010) have reported this event in the Mediterranean basin as the FO of *Reticulofenestra zancleana,* a junior synonym of *Reticulefenestra cisnerosii* (Lancis, 1998; Lancis and Flores, 2006). This form is frequent in the sections studied (see graphs Fig. 7). Its FO is coincident with the FO of *C. acutus* in the Mediterranean. Its absence in the conglomeratic levels of the bottom of the PE section is due to its particular sedimentary environment. Its LO slightly predates the first occurrence of *Discoaster tamalis* and the FCO of *Discoaster asymmetricus*.

The FO of *Ceratolithus rugosus* marks the base of the CN10c subzone (Okada and Bukry, 1980) and the NN13 zone (Martini, 1971) occurring in the Equatorial Atlantic during the C3n.4n (Thvera) chron at 5.05Ma, and in the Equatorial Pacific at 5.12Ma (Backman and Raffi, 1997; Lourens *et al.*, 2004; Raffi *et al.*, 2006). It is also a rare event in the Mediterranean. Thus, Rio *et al.* (1990) used the drop in abundance of the fairly continuous *Amaurolithus* spp., and the FO of *Helicosphaera sellii* (the increase in the species to a frequency >1% in a count of 100 helicoliths) in their Mediterranean biostratigraphic scheme to mark the bottom of their MNN13 zone. Our data confirm the

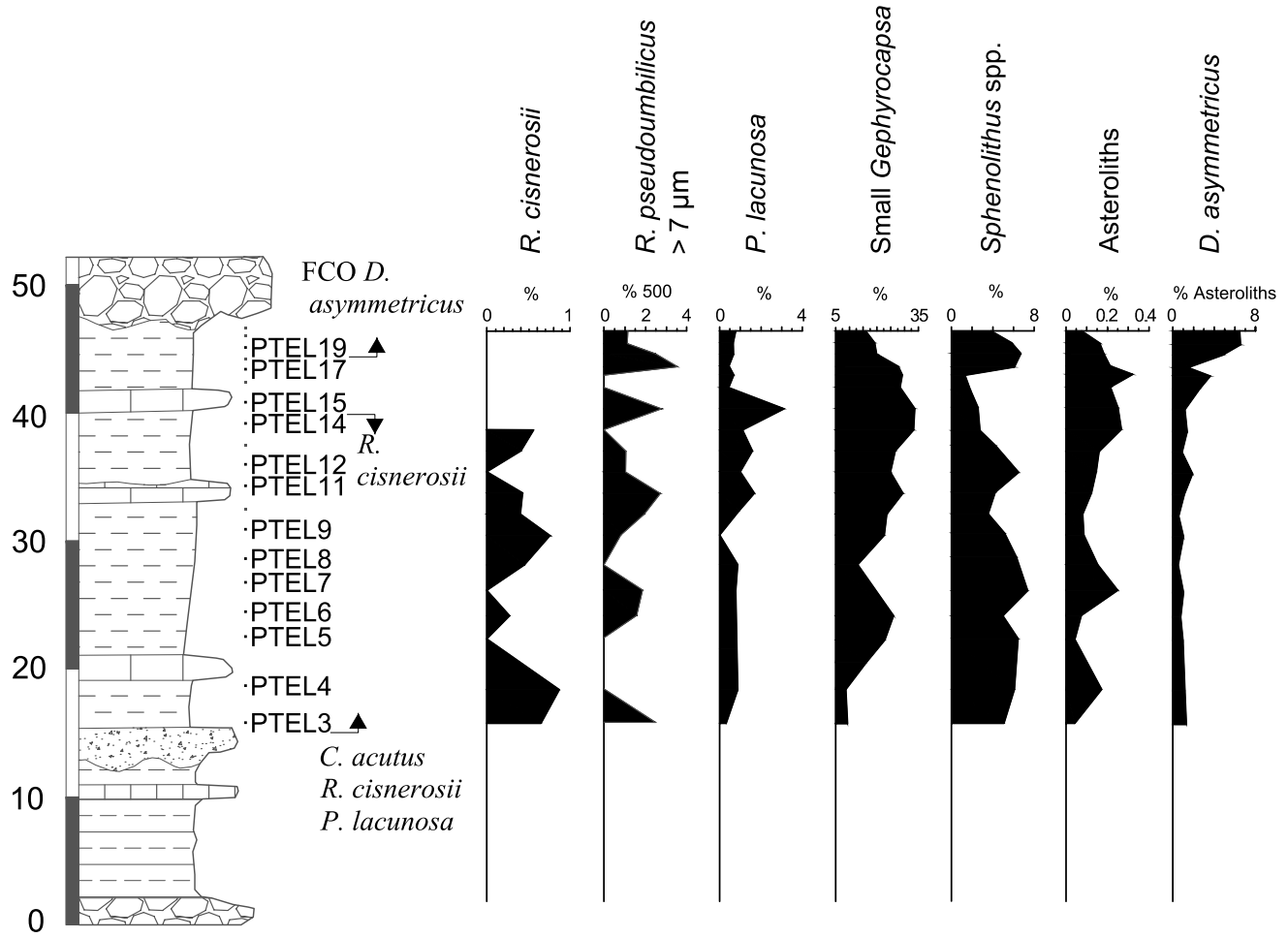

FIGURE 7. Quantitative distribution patterns of selected nannofossils in the Pantano de Elche (PTEL) section. Percentages are relative to 500 specimens >3µm counted (500 %). The percentage of "small *Gephyrocapsa*" is calculated relative to all the nanoliths (%). The *Discoaster tamalis* and *Discoaster asymmetricus* percentage is calculated relative to all the asteroliths (asteroliths %). See section Methods. Note differences in scaling.

scarcity of *C. rugosus* since we found it only sporadically in the DPH, SM, and GUA sections.

Rio (1982) reported an increase in "small *Gephyrocapsa* spp." in the Mediterranean Sea around 3.5 to 3.6Ma. Dermitzakis and Theodoridis (1978) observed the first forms at the bottom of the NN13 of Martini (1971). Driever (1988), Lourens *et al.* (1996), and Lourens *et al.* (2004) established an age of 4.33Ma for the FO of "small *Gephyrocapsa* spp." for the Mediterranean, and found it slightly below the FCO of *D. asymmetricus*. In our sections, this event is found to almost coincide with the FO of *C. rugosus*, at the bottom of the NN13 zone (Martini, 1971).

The appearance of *Pseudoemiliana lacunosa* in the stratigraphic record is not normally used in current calcareous nannofossil biostratigraphic schemes because of discrepancies regarding its FO among the different investigators. Gartner (1969), Raffi and Rio (1979), Martini (1979), and Young *et al.* (1994) place the FO of *Pseudoemiliania lacunosa* close to the LO of *Reticulofenestra pseudoumbilicus* in the NN15 zone (Martini, 1971). For Rio *et al.* (1990) and Raffi *et al.* (2006) *P. lacunosa* appears with low frequency between the FCO of *D. asymmetricus*, and the LO of *R. pseudoumbilicus*. By contrast, Driever (1988) and Dermitzakis and Theodoridis (1978) observed it from the base of the NN13 zone (Martini, 1971). In our samples the FO of *Pseudoemiliania lacunosa* was found slightly above the FO of *C. rugosus* and can thus be included in the NN13 zone (Martini, 1971), this FO being an easily recognizable and useful event in the Eastern Betic basins for correlation purposes.

The FCO of *D. asymmetricus* marks the boundary between the NN13 and the NN14 zones (Martini, 1971), and also between the CN11a and the CN11b zones (Okada and Bukry, 1980). Rio *et al.* (1990) have defined this event as the point at which *D. asymmetricus* reached a >5% frequency in a count of 100 discoasters

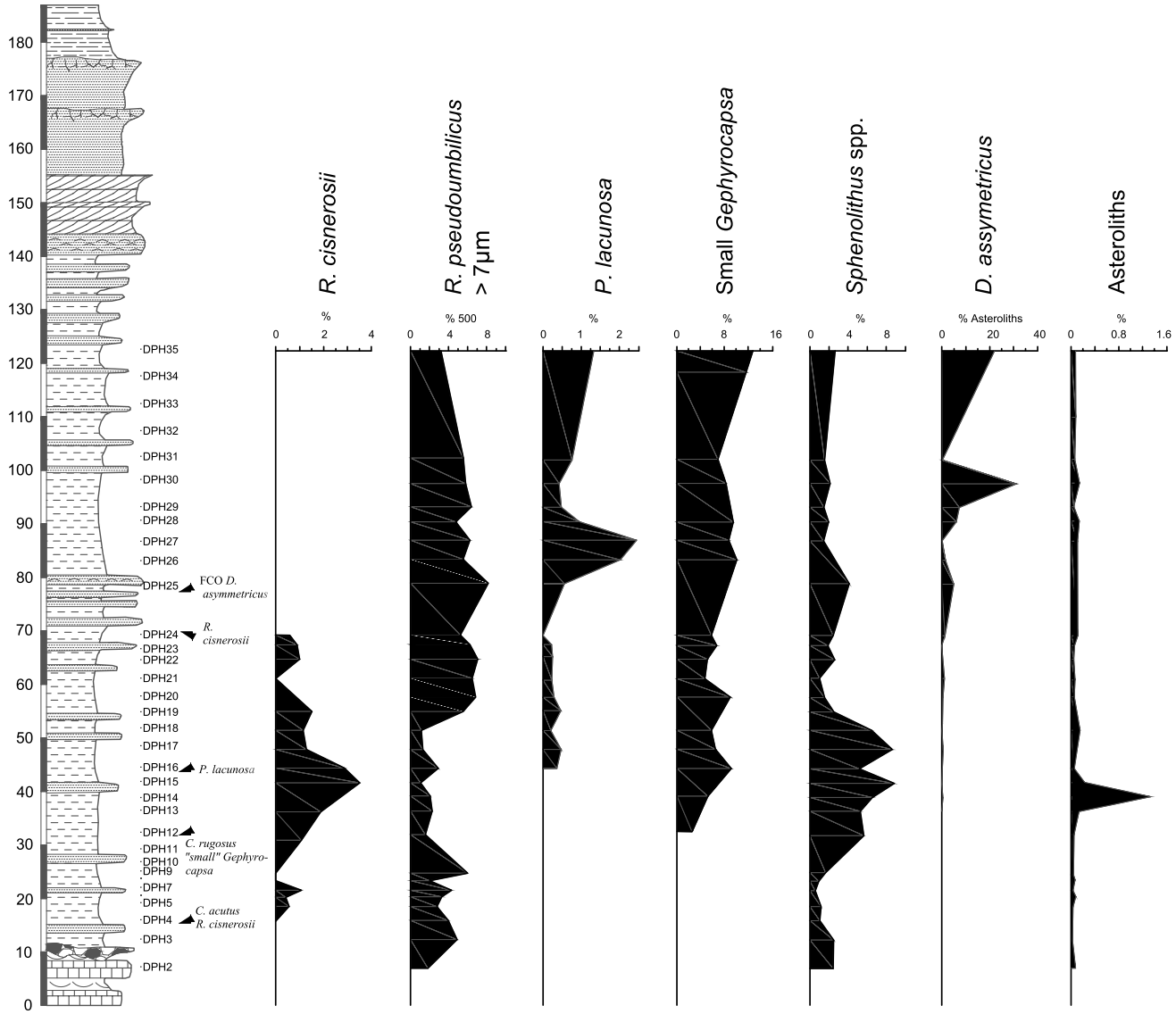

FIGURE 8. Quantitative distribution pattern of selected nannofossils in the Dehesa de Pino Hermoso (DPH) section. Percentages are relative to 500 specimens >3µm counted (500%). The percentage of "small *Gephyrocapsa*" is calculated relative to all the nanoliths (%). The *Discoaster tamalis* and *Discoaster asymmetricus* percentage is calculated relative to all the asteroliths (asteroliths %). See section Methods. Note differences in scaling.

and they used it as the boundary between their MNN13 and the MNN14 zones. In the Mediterranean, Rio *et al*. (1990) observed this event just above the C3n.1n subchron. Recently, in the Equatorial Pacific FCO of *D. asymmetricus* has been dated at 4.13Ma (Raffi and Flores, 1995; Shackleton *et al*., 1995) and in the Mediterranean at 4.12Ma (Lourens *et al*., 1996; Driever, 1988; Lourens *et al*., 2004). The DPH and PTEL sections exhibit this event, and the GUA and SP sections record *D. asymmetricus* from the bottom.

It is hard to establish the FO of *Discoaster tamalis* owing to the scarcity of this form in the samples. For the Mediterranean it is calibrated at 3.97Ma (Lourens *et al*., 2004), slightly younger than the FCO of *D. asymmetricus*. The FO of *D. tamalis* is found in the GUA and SP sections.

Raffi and Rio (1979) and Rio *et al*. (1990) placed the LO of *R. pseudoumbilicus* in the sample in which frequency of the species, for forms larger than 7*µ*m, was below 2% of the total assemblage in a count of 500 nannofossil specimens. However, as mentioned by Rio *et al*. (1990) its detection in the sections is complicated owing to reworking. This event appears in the GUA section below the LO of *Spenolithus* spp. It also marks the boundary between the NN15 and the NN16 zones of Martini (1971), and the CN11b and the CN12aA zones of Okada and Bukry (1980) and has been

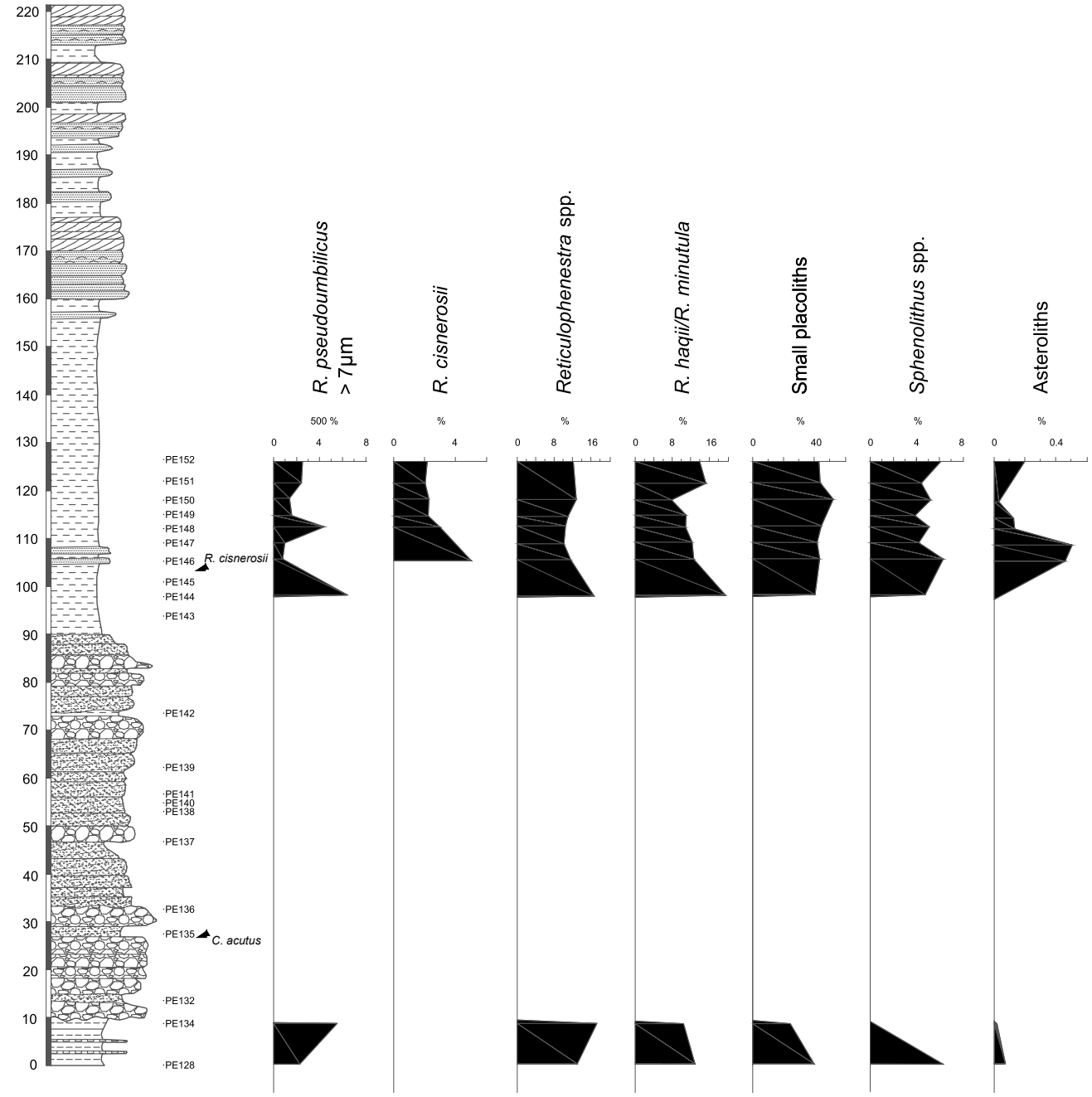

FIGURE 9. Quantitative distribution pattern of selected nannofossils in the Embalse la Pedrera (PE) section. Percentages are relative to 500 specimens >3µm counted (500%). The percentage of "small *Gephyrocapsa*" is calculated relative to all the nanoliths (%). See section Methods. Note differences in scaling.

calibrated in the Mediterranean at 3.84Ma (Lourens *et al.*, 1996; Lourens *et al.*, 2004; Raffi *et al.*, 2006).

The last event is the LO of *Sphenolithus* spp., occurring above the LO of *R. psedoumbilicus*. It has been used to split the lower CN12a into CN12aA/CN12aB (Okada and Bukry, 1980 emend. Bukry, 1991). The LO of *Sphenolithus* spp. has been calibrated at 3.65Ma in the Equatorial Pacific (Raffi and Flores, 1995; Shackleton *et al.*, 1995; Lourens *et al.*, 2004; Raffi *et al.*, 2006), and at 3.52–3.56Ma in the Equatorial Atlantic (Raffi *et al.*, 2006). It has been found in the uppermost part of the GUA section.

Sequence dating

From bottom to top, the events recognized in the lower sequence, including the paleo-valley fill (Pedrera Formation), the lower Hurchillo marls and the lower

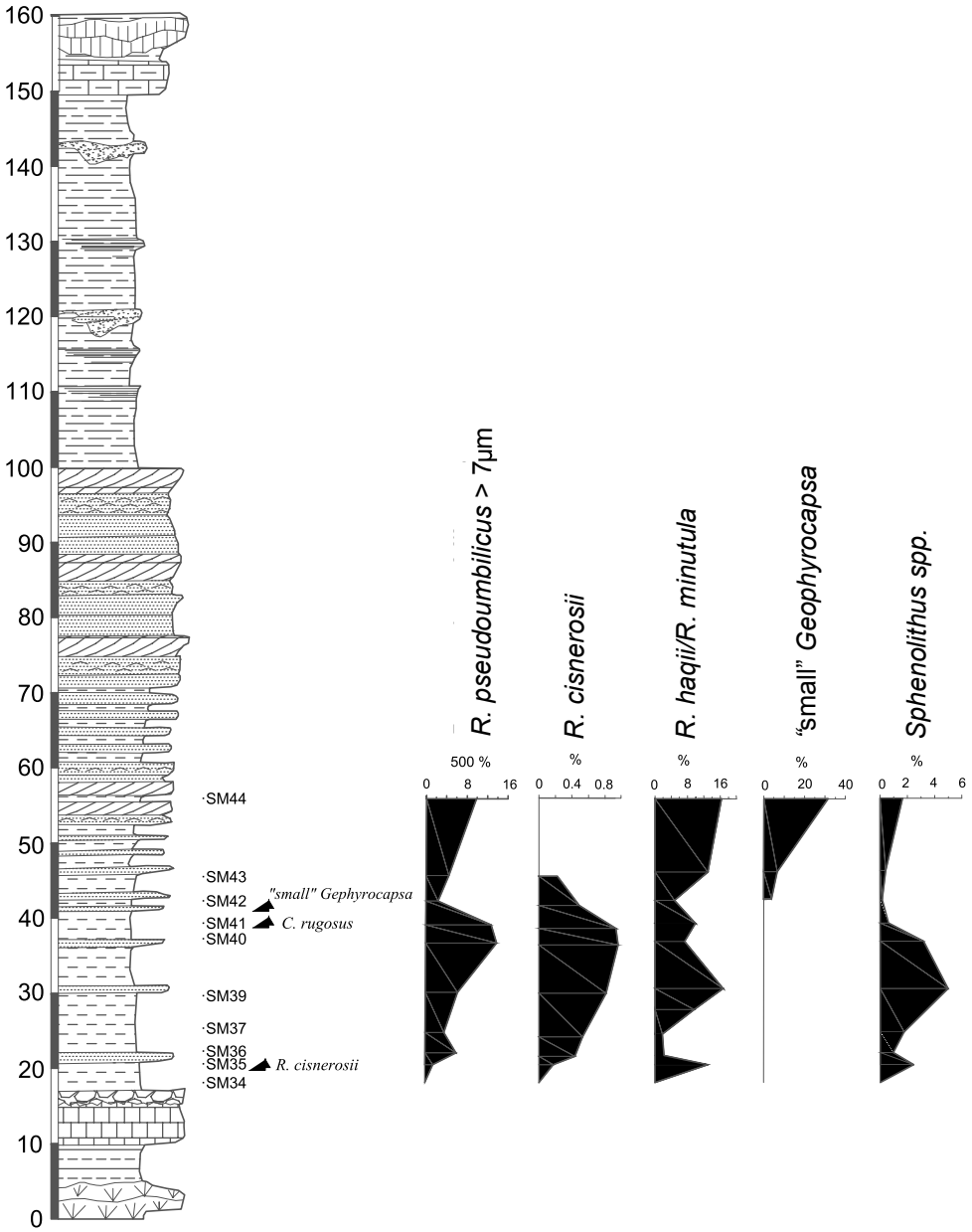

FIGURE 10. Quantitative distribution pattern of selected nannofossils in the San Miguel (SM) section. Percentages are relative to 500 specimens >3µm counted (500%). The percentage of "small *Gephyrocapsa*" is calculated relative to all the nanoliths (%). See section Methods. Note differences in scaling.

yellow calcareous sandstone are (Figs. 3; 4; 5): i) the FO of *Ceratolithus acutus*; ii) the FO of *Reticulofenestra cisnerosii*; iii) the FO of *Ceratolithus rugosus*; iv) the FO of "small *Gephyrocapsa* spp."; v) the FO of *Pseudoemiliana lacunosa*; vi) the LO of *R. cisnerosii* and vii) the FCO of *Discoaster asymmetricus*. These allow it to be situated in the NN12-NN14 biozones of Martini (1971), the CN10b-CN11b zones of Okada and Bukry (1980), and the MNN12b-MNN14 zones of Rio *et al.* (1990).

The upper sequence, including the upper Hurchillo marls and the upper yellow calcareous sandstone, yields: viii) the FO of *Discoaster tamalis*; iv) the LO of *Reticulofenestra pseudoumbilicus* and x) the LO of *Sphenolithus* spp. This sequence can be dated as the upper part of NN15-NN16 of Martini (1971), CN11b-CN12a of Okada and Bukry (1980), and MNN15 to MNN16 of Rio *et al.* (1990).

Both sequences can be considered as Highstand System Tracts and the boundary between them a relative sea-level fall. The top of the lower sequence has at least two emersion episodes (see the Transgressive Pliocene header description of PE, SM, and DPH). The data on the Bajo Segura indicate that the discontinuity between both

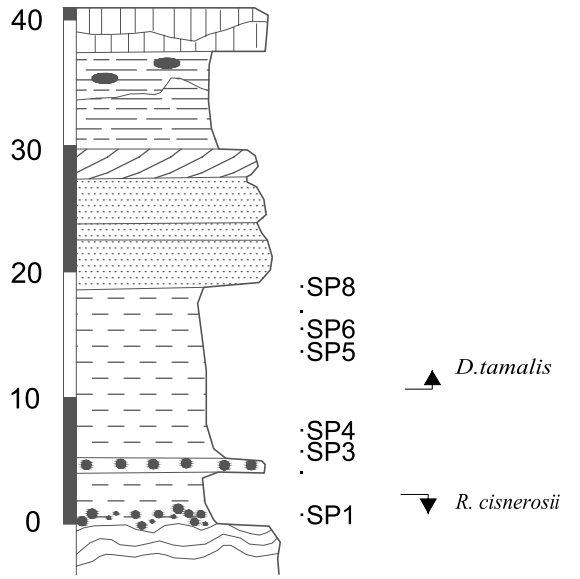

FIGURE 11. Santa Pola (SP) section with the location of samples and nannofossil events.

sequences could be calibrated as the upper part of the NN14 to the middle part of the NN15 of Martini (1971), within the CN11b of Okada and Bukry (1980), and also the upper part of the MNN14 to the middle part of the MNN15 of Rio *et al.* (1990) (Fig. 3). The sequence boundary occur after the FCO of *Discoaster asymmetricus* found in the uppermost sediments of the lower sequence and before the FO of *Discoaster tamalis* in the lowermost part of the upper sequence. Thus the age of this sequence boundary can be estimated between 4.1 and 4.0Ma ago.

PALEOECOLOGICAL CONSIDERATIONS

Coccolithophore abundances (Figs. 6; 7; 8; 9; 10; 11) were used to reconstruct the paleoenvironmental conditions of the Early Pliocene in the basin. The abundance of *R. pseudoumbilicus* and asteroliths has been related to warm and relatively deep water (Bukry, 1981; Rio and Sproveri, 1986; Driever, 1988; Rio *et al.*, 1990; Lancis, 1998). Additionally, the intermediate and small reticulofenestrid forms indicate the proximity of the coast. The lower parts of both sequences point to these relatively open marine conditions and an upward-trending restriction.

CORRELATION WITH OFFSHORE DATA

Many authors (Rabineau, 2001; Lofi *et al.*, 2003; 2005; Gorini *et al.*, 2005; Duvail *et al.*, 2005; Garcia *et al.*, 2011; Urgeles *et al.*, 2011; Martínez del Olmo, 2011b; Leroux, 2013), using the seismic lines around the Western Mediterranean Basin, have described the post-Messinian sediments as multi-hectometric prograding prisms. The offshore study of the thick Early Pliocene sediments filling the MES in the Gulf of Lion by Lofi *et al.* (2003) differentiated a major prograding seismic unit U1, divided into two seismic subunits (U1-a, the lower, and U1-b) deposited beneath the modern inner to middle shelf, showing a shallowing-upward trend with a major upper boundary interpreted as a major erosional unconformity formed during a relative fall in sea-level. Leroux (2013) correlates the sequence boundary between both seismic subunits with the p7 reflector of Rabineau (2001), and the Pr6 reflector of Duvail *et al.* (2005) of the Gulf of Lion (Fig. 3). The sediments included in the U1-a seismic unit of Lofi *et al.* (2003) have been mapped by Leroux (2013, Messinian top to p7 sediments), showing that they are restricted to depths between 100 to 2000 m below today sea-level in the Gulf of Lion.

From well data by Lofi *et al.* (2003), U1 was dated as Early Pliocene, but not ruling out the earliest Late Pliocene. The age boundary between both seismic subunits is not sufficiently well constrained, being estimated by Lofi *et al.* (2003) to lie between the MPL2 to MPL3 planktonic foraminifera biozones (Lourens *et al.*, 2004). Considering both, the Gulf of Lion seismic subunits as well as the Bajo Segura sedimentary units filling up the MES, a correlation between them could be proposed. The lower Hurchillo sedimentary cycle may be the onland equivalent of the U1-a seismic unit and the upper Hurchillo sedimentary cycle that of U1-b seismic unit (Fig. 3).

The age of the U1 seismic unit mainly coincides with the set of the two Bajo Segura sedimentary units but the age boundary between the two seismic subunits proposed by Lofi *et al.* (2003) seems to be about 0.5Ma older than the boundary between the two Bajo Segura sedimentary units. This could be explained in terms of the intrinsic errors arising from the broad correlation between the seismic units and the well data used in the dating of the U1 subunits (Lofi *et al.*, 2003). The sequence boundary between the two Bajo Segura sedimentary units could be correlated with the Za1-Za2 sequence boundary (Snedden and Liu, 2011). Since the U1 has been dated as Lower Pliocene, the fall in sea-level that occurred around its upper boundary could have been close to the Lower to Upper Pliocene boundary (Lofi *et al.*, 2003). However, in the Bajo Segura Basin above the upper Hurchillo marls further marine sedimentation is only recorded in the high sea-levels during the Quaternary, such as the Holocene (Soria *et al.*, 1999).

DISCUSSION

The lowermost Pliocene sediments correspond to a high-energy paleo-valley fill (García-García *et al.*, 2011). Outside

the paleo-valley, where the MES is exposed as a gentle basin-scale surface, a wide hiatus separates the transgressive Pliocene deposits from the Messinian ones. The most seaward section, the GUA, and the seaward and elevated portions of the paleorelief, seen at SP, show a glauconitic level (Lancis *et al.*, 2004b), that may be interpreted as condensed sections with a low sedimentation rate. These levels mark areas of the basin where the oceanic currents winnowed the coccoliths. This could explain the absence of the earliest Pliocene nannofossil bioevents in the GUA and SP sections. The PE and DPH are the most proximal sections studied in this work and they show the upper sequence to be more transgressive over the lower coastline, as seen in the seismic profiles (see Lofi *et al.*, 2003). At this point, no quantification of the landward migration of the coastline in the upper transgression can be estimated because of the uncertainties about the rate of sea-level increase in an anomalous environment with high subsidence (after extensive flooding of the platforms), and with a highly available sediment supply (after the increased erosion of the Mediterranean landscapes during the Messinian). Additionally, the SM section shows thinner upper Huchillo marls, probably due to a local uplift of this section, located in a hinge of an anticline (Soria *et al.*, 2008a), which would have compensated the second marine transgression.

CONCLUSIONS

Six stratigraphic sections located in key points of the Bajo Segura Basin show that the base of the Lower Pliocene sediments resting on the MES are diachronous. These sediments correspond to two transgressive-regressive sequences, the lower Hurchillo sedimentary cycle and the upper Hurchillo sedimentary cycle. These two transgressive-regressive sequences can be correlated with the two lower Pliocene seismic sequences infilling the inner to middle Gulf of Lion shelf on the Western Mediterranean (Lofi *et al.*, 2003; Leroux, 2013). The upper transgression arrived farther inland than the lower one. Future work should focus on explaining the cause of this younger Early Pliocene transgression and quantifying the coastline migration.

ACKNOWLEDGMENTS

D. Violanti is acknowledged for comments on an early version of this paper. We would like to acknowledge also the editor M. Garcés and two anonymous referees for some interesting suggestions. This work has been supported by projects: CGL2007-65832/BTE Ministerio de Educación y Ciencia, CGL2009-07830/BTE Ministerio de Ciencia e Innovación, and PASUR.CGL2009-08651 Ministerio de Ciencia e Innovación Projects and BEST/2010/068 Generalitat Valenciana.

REFERENCES

Bache, F., 2008. Evolution Oligo-Miocène des Marges du Micro Océan Liguro-Provençal. PhD Thesis. Université de Bretagne Occidentale, 328pp.

Bache, F., Olivet, J.-L., Gorini, C., Aslanian, D., Labails, C., Rabineau, M., 2010. Evolution of rifted continental margins: the case of the Gulf of Lions (Western Mediterranean Basin). Earth and Planetary Science Letters, 292, 345-356.

Bache, F., Olivet, J.L., Gorini, C., Rabineau, M., Baztan, J., Aslanian, D., Suc, J.-P., 2009. Messinian erosional and salinity crises: view from the Provence Basin (Gulf of Lions, Western Mediterranean). Earth and Planetary Science Letters, 286, 139-157. DOI: 10.1016/j.epsl.2009.06.021

Bache, F., Popescu, S.-M., Rabineau, M., Gorini, C., Suc, J.-P., Clauzon, G., Olivet, J.-L., Rubino, J.-L., Melinte-Dobrinescu, M.C., Estrada, F., Londeix, L., Armijo, R., Meyer, B., Jolivet, L., Jouannic, G., Leroux, E., Aslanian, D., Tadeu Dos Reis, A., Mocochain, L., Dumurdžanov, N., Zagorchev, I., Lesić, V., Tomić, D., Çağatay, M.N., Brun, J.-P., Sokoutis, D., Csato, I., Ucarkus, G., Çakır, Z., 2012. A two-step process for the reflooding of the Mediterranean basin after the Messinian Salinity Crisis. Basin Research, 24(2), 125-153. DOI: 10.1111/j.1365-2117.2011.00521.x

Backman, J., Raffi, I., 1997. Calibration of Miocene nannofossil events to orbitally-tuned cyclostratigraphies from Ceara Rise. In: Shackelton, N.J., Curry, W.B., Richter, C., Bralower, T.J. (eds.). Proceedings of the Ocean Drilling Program, Scientific Results, 154, 83-99. DOI: 10.2973/odp.proc.sr.154.101.1997

Bukry, D., 1975. Coccolith and Silicoflagellate Stratigraphy, Northwestern Pacific Ocean, Deep Sea Drilling Project, Leg 32. In: Larson, R.L., Moberly, R., *et al.* (eds.). Initial Reports of the Deep Sea Drilling Project, 32, 677-701. DOI: 10.2973/dsdp.proc.32.124.1975

Bukry, D., 1991. Paleoecological transect of Western Pacific Ocean late Pliocene coccolith flora. Part I: Tropical Ontong-Java Plateau at ODP 806B. Open Republic – U. S. Geological Survey, 91-552, 35p.

Calvet, F., Zamarreño, I., Vallés, D., 1996. Late Miocene reefs of the Alicante-Elche basin, southeast Spain. In: Models for Carbonate stratigraphy from Miocene reef complexes of Mediterranean regions, Society of Economic Paleontologists and Mineralogists Tulsa, 177-190.

Caracuel, J.E., Soria, J.M., Yébenes, A., 2004. Early Pliocene transgressive coastal lags (Bajo Segura Basin, Spain): a marker of the flooding after the Messinian salinity crisis. Sedimentary Geology, 169, 121-128.

Caracuel, J.E., Corbí, H., Giannetti, A., Monaco, P., Soria, J.M., Tent-Manclús, J.E., Yébenes, A., 2011. Paleoenvironmental changes during the Late Miocene (Messinian)-Pliocene transition (Bajo Segura Basin, Southeastern Spain): Sedimentological and ichnological evidence. Palaios, 26, 754-766. DOI: 10.2110/palo.2011.p11-016r

Castradori, D., 1998. Calcareous nannofossils in the basal Zanclean of eastern Mediterranean Sea: remarks on paleoceanography

and sapropel formation. In: Robertson, A.H.F., Emeis, K.-C., Richter, C., Camerlenghi, A. (eds.). Proceedings of the Ocean Drilling Program, Scientific Results, 160, 113-123. DOI: 10.2973/odp.proc.sr.160.005.1998

Cita, M.B., Gartner, S., 1973. Studi sul Pliocene e gli strati di passagio dal Miocene al Pliocene, IV. The stratotype Zanclean foraminiferal and nannofossil biostratigraphy. Rivista Italiana di Paleontologia e Stratigraphia, 79, 503-558.

Cita, M.B., Ryan, W.B.F., 1978. Messinian erosional surfaces in the Mediterranean. Marine Geology, 27, 193-365.

Clauzon, G., Aguilar, J.-P., Michaux, J., 1987. Le basin pliocène du Roussillon (Pyrénées-Orientales, France): exemple d'évolution géodynamique d'une ria consécutive à la crise de salinité messinienne. Comptes Rendus de l'Académie de Sciences, Paris, II 304, 385-390.

Corbí Sevila, H.A., 2010. Los foraminíferos de la Cuenca neógena del Bajo Segura (Sureste de España): biostratigrafía y cambios paleoambientales en relación con la crisis de salinidad del Mediterráneo. PhD Thesis, Universidad de Alicante, 280pp.

De Larouzière, F.D., Bolze, J., Bordet, P., Hernandez, J., Montenat, C., Ott d'Estevou, P., 1988. The Betic segment of the lithospheric Trans-Alboran shear zone during the Late Miocene. Tectonophysics, 152, 41-52.

Dermitzakis, M.D., Theodoridis, S.A., 1978. Planktonic Foraminifera and Calcareous nanoplankton from the Pliocene of Koufonisi Island (East Crete, Greece). Annales Géologiques des Pays Helléniques, 29, 630-643.

Di Stefano, A., Sturiale, G., 2010. Refinements of calcareous nannofossil biostratigraphy at the Miocene/Pliocene Boundary in the Mediterranean region. Geobios, 43, 5-20. DOI: 10.1016/j.geobios.2009.06.007

Driever, B.W.H., 1988. Calcareous nanofossil biostratigraphy and Paleoenvironmental interpretation of the Mediterranean Pliocene. Utrecht Micropaleotology Bulletin, 36, 1-245.

Duvail, C., Gorini, C., Lofi, J., Le Strat, P., Clauzon, G., Tadeu dos Reis, A., 2005. Correlation between onshore and offshore Pliocene-Quaternary systems tracts below the Roussillon Basin (eastern Pyrenees, France). Marine and Petroleum Geology, 22, 747-756. DOI: 10.1016/j.marpetgeo.2005.03.009

Fallot, P., 1948. Les Cordillères bétiques. Estudios Geológicos, 8, 83-172.

Feldmann, M., McKenzie, J., 1997. Messinian stromatolite-thrombolite associations, Santa Pola, SE Spain: an analogue for the Palaeozoic? Sedimentology, 44, 893-914.

García, M., Maillard, A., Aslanian, D., Rabineau, M., Alonso, B., Gorini, C., Estrada, F., 2011. The Catalan margin during the Messinian Salinity Crisis: Physiography, morphology and sedimentary record. Marine Geology, 284(1-4), 158-174. DOI: 10.1016/j.margeo.2011.03.017

García-García, F., Corbí, H., Soria, J.M., Viseras, C., 2011. Architecture analysis of a river flood-dominated delta during an overall sea-level rise (early Pliocene, SE Spain). Sedimentary Geology, 237, 102-113. DOI: 10.1016/j.sedgeo.2011.02.010

Gartner, Jr. S., 1969. Correlation of Neogene planktonic foraminifera and calcareous nannoplankton zones. Transactions of the Gulf Coast Association of Geological Societies 19, 585-599.

Gartner, S., Bukry, D., 1974. *Ceratolithus acutus* Gartner and Bukry n. sp. and *Ceratolithus amplificus* Bukry and Percival, nomenclatural classification. Tulane Studies, Geology and Paleontology, 11, 115-118.

Haq, B.U., Hardenbol, J., Vail, P.R., 1987. Cronology of fluctuating sea levels since the Triassic. Science, 235, 1156-1167.

Hilgen, F.J., Lourens, L.J., Van Dam, J.A., 2012. The Neogene Period. In: Grandstein, F.M., Ogg, J.G., Schmitz, M., Ogg, G. (eds.). The Geologic Time Scale 2012. Elsevier, 923-978. DOI: 10.1016/B978-0-444-59425-9.000 29-9

Lancis, C., 1998. El nanoplancton calcáreo de las cuencas béticas orientales. PhD Thesis. Universidad de Alicante, 423pp.

Lancis, C., Flores, J.A., 2006. A new biostratigraphically significant calcareous nannofossil species in the Early Pliocene of Mediterranean. Micropaleontology, 52(5), 477-481. DOI: 10.2113/gsmicropal.52.5.477

Lancis, C., Flores, J.A., Sierro, F., Estévez, A., 2004a. Análisis biostratigráfico mediante el empleo de nanofósiles calcáreos en la cuenca neógena de San Miguel-Torremendo (Cordillera Bética Oriental). Geo-Temas, 7, 257-262.

Lancis, C., Yébenes, A., Flores, J.A., Tent-Manclús, J.E., 2004b. Precisiones bioestratigráficas y sedimentológicas sobre el Plioceno del norte de la Sierra de Santa Pola (Alicante). Geo-Temas, 7, 143-147.

Leroux, E. 2013. Quantification des flux sédimentaires et de la subsidence du bassin Provençal. PhD Thesis, Université de Brest, 455pp.

Lofi, J., Gorini, C., Berné, S., Clauzon, G., Tadeu Dos Reis, A., Ryan, W.B.F., Steckler, M.S., 2005. Erosional processes and paleo-environmental changes in the Western Gulf of Lions (SW France) during the Messinian Salinity Crisis. Marine Geology, 217, 1-30. DOI: 10.1016/j.margeo.2005.02.014

Lofi, J., Rabineau, M., Gorini, C., Berne, S., Clauzon, G., De Clarens, P., Tadeu Dos Reis, A., Mountain, G.S., Ryan, W.B.F., Steckler, M.S., Fouchet, C., 2003. Plio-Quaternary prograding clinoform wedges of the western Gulf of Lion continental margin (NW Mediterranean) after the Messinian Salinity Crisis. Marine Geology, 198, 289-317. DOI: 10.1016/S0025-3227(03)00120-8

Lofi, J., Sage, F., Déverchère, J., Loncke, L., Maillard, A., Gaullier, V., Thinon, I., Gillet, H., Guennoc, P., Gorini, C., 2011. Refining our knowledge of the Messinian Salinity Crisis records in the offshore domain through Multi-site seismic analysis. Bulletin de la Société géologique de France, 182(2), 163-180. DOI: 10.2113/gssgfbull.182.2.163

Lourens, L.J., Hilgen, F.J., Raffi, I., Vergnaud-Grazzini, C., 1996. Early Pleistocene chronology of the Vrica section (Calabria, Italy). Paleoceanography, 11, 797-812.

Lourens, L.J., Hilgen, F., Shackleton, N.J., Laskar, J., Wilson, D., 2004. The Neogene period. In: Gradstein, F.M., Ogg,

J.G., Smith, A.G. (eds.). A Geologic Time Scale. Cambridge University Press, 409-440.

Martínez del Olmo, W., 2011a. El Arrecife messiniense del sondeo Torrevieja Marino C-1 desde las líneas sísmicas (SE. de España). Revista de la Sociedad Geológica de España, 24, 173-185.

Martínez del Olmo, W., 2011b. El Messiniense en el Golfo de Valencia y el Mar de Alborán. Revista de la Sociedad Geológica de España, 24, 237-257.

Martini, E., 1971. Standard Terciary and Quaternary calcareous nannoplankton zonation. Proceedings II Planktonic conference, Tecnoscienza, Roma, 2, 736-785.

Martini, E., 1979. Calcareous Nannoplankton and Silicoflagellate Biostratigraphy at Reykjakes Ridge, Northeastern North Atlantic (DSDP Leg 49, sites 407 and 409). In: Luyendyk, B.P., Cann, J.R., Duffield, W.A., Faller, A.M., Kobayashi, K., Poore, R.Z., Roberts, W.P., Sharman, G., Shor, A.N., Steiner, M., Steinmetz, J.C. Varet, J., Vennum, W., Wood, D.A., Zolotarev, B.P. (eds.). Initial Reports of the Deep Sea Drilling Project 49, Washington (U.S. Goverment Printing Office), 533-549. DOI: 10.2973/dsdp.proc.49.117.1979

Maillard, A., Hübscher, C., Benkhelil, J., Tahchi, E., 2011. Deformed Messinian markers in the Cyprus Arc: tectonic and/or Messinian Salinity Crisis indicators? Basin Research, 23(2), 146-170. DOI: 10.1111/j.1365-2117.2010.00464.x

Montenat, C., 1977. Les bassins néogènes du levant d'Alicante et de Murcia (Cordillères bétiques orientales- Espagne). Stratigraphie, paléogéographie et évolution dynamique. Documents Laboratoire Géologie Faculté des Sciences de Lyon, 69, 345pp.

Montenat, C., Ott d'Estevou, Ph., Coppier, G., 1990. Les basins neogenes entre Alicante et Cartagena. In: Montenat, C. (ed.). Les Bassins Néogènes du Domaine Bétique Orientale (Espagne). Documents et Travaux, Institut Géologique Albert de Lapparent, 12-13, 313-368.

Okada, H., Bukry, D., 1980. Supplementary modification and introduction of code numbers to the low-latitude coccolith biostratigraphic zonation (Bukry, 1973; 1975). Marine Micropaleontology, 5, 321-325.

Rabineau, M. 2001. Un modèle géométrique et stratigraphique des séquences de dépôts quaternaires sur la marge du Golfe du Lion: Enregistrement des cycles climatiques de 100 000 ans. PhD Thesis. Université de Rennes 1, 392pp.

Raffi, I., Backman, J., Fornaciari, E., Pälike, H., Rio, D., Lourens, L., Hilgen, F., 2006. A review of calcareous nannofossil astrobiochronology encompassing the past 25 million years. Quaternary Science Reviews, 25, 3113-3137. DOI: 10.1016/j.quascirev.2006.07.007

Raffi, I., Rio, D., 1979. Calcareous Nannofossils biostratigraphy of DSDP site 132, Leg 13 (Tyrrhenian sea), western Mediterranean. Rivista Italiana di Paleontologia e Stratigrafia, 85(1), 127-172.

Rio, D., 1982. The Fossil distribution of coccolithophore genus *Gephyrocapsa* Kamptner and related Plio-Pleistocene chronostratigraphic problems. In: Prell, W.L., Gardner, J.V., *et al.* (eds.). Initial Reports of the Deep Sea Drilling Project, 68, 325-343. DOI: 10.2973/dsdp.proc.68.109.1982

Rio, D., Raffi, I., Villa, G., 1990. Pliocene–Pleistocene calcareous nannofossil distribution patterns in the western Mediterranean. In Kastens, K.A., Mascle, J., *et al.* (eds.). Proceedings of the Ocean Drilling Program, Scientific Results, 107, 513-533. DOI: 10.2973/odp.proc.sr.107.164.1990

Roveri, M., Lugli, S., Manzi, V., Gennari, R., Iaccarino, S.M., Grossi, F., Taviani, M., 2006. The record of Messinian events in the Northern Apennines foredeep basins. Acta naturalia de l'Ateneo Parmese, 42(3), 47-122.

Ryan, W.B.F., Hsü, K.J., Cita, M.B., Dumitrica, P., Lort, J.M., Maync, W., Nesteroff, W.D., Paulot, G., Stradner, H., Wezel, F.C., 1973. Initial Reports of the Deep Sea Drilling Project, 13, Washington (U.S. Goverment Printing Office), 514-1447pp. DOI: 10.2973/dsdp.proc.13.1973

Shackleton, N.J., Crowhurst, S., 1997. Sediment fluxes based on an orbitally tuned time scale 5Ma to 14Ma, Site 926. In: Shackleton, N.J., Curry, W.B., Richte, C., Bralower, T.J. (eds.). Proceedings of the Ocean Drilling Program, Scientific Results, 154, 69-82. DOI: 10.2973/odp.proc.sr.154.102.1997

Shackleton, N.J., Hall, M.A., Pate, D., 1995. Pliocene stable isotope stratigraphy of Site 846. In: Pisias, N.G., Mayer, L.A., Janacek, T.R., Palmer-Julson, A., van Andel, T.H. (eds.). Proceedings of the Ocean Drilling Program, Scientific Results, 138, 337-355. DOI: 10.2973/odp.proc.sr.138.117.1995

Snedden, J.W., Liu, C., 2011. Recommendations for a uniform chronostratigraphic designation system for Phanerozoic depositional sequences. American Asssociation of Petroleum Geologists Bulletin, 95, 1095-1122.

Soria, J.M., Alfaro, P., Estévez, A., Delgado, J., Durán, J.J., 1999. The Holocene sedimentation rates in the Lower Segura Basin (eastern Betic Cordillera, Spain): eustatic implications. Bulletin Société Géologique de France, 170, 349-354.

Soria, J.M., Alfaro, P., Ruiz Bustos, A., Serrano, F., 1996. Organización estratigráfica y biostratigráfica del Plioceno en el borde sur de la Cuenca del Bajo Segura (sector de Rojales, Alicante), Cordillera Bética oriental. Estudios Geológicos, 52, 137-145.

Soria, J.M., Caracuel, J.E., Corbí, H., Dinarès-Turell, J., Lancis, C., Tent-Manclús, J.E., Viseras, C., Yébenes, A., 2008a. The Messinian-early Pliocene stratigraphic record in the southern Bajo Segura Basin (Betic Cordillera, Spain): Implications for the Mediterranean salinity crisis. Sedimentary Geology, 203, 267-288. DOI: 10.1016/j.sedgeo.2007.12.006

Soria, J.M., Caracuel, J.E., Corbí, H., Dinarès-Turell, J., Lancis, C., Tent-Manclús, J.E., Yébenes, A., 2008b. The Bajo Segura Basin (SE Spain): implications for the Messinian Salinity Crisis in the Mediterranean margins. Stratigraphy, 5(3-4), 259-265.

Soria, J.M., Caracuel, J.E., Yébenes, A., Fernández, J., Viseras, C., 2005. The stratigraphic record of the Messinian salinity crisis in the northern margin of the Bajo Segura Basin (SE Spain). Sedimentary Geology, 179, 225-247.

Urgeles, R., Camerlenghi, A., García-Castellanos, D., De Mol, B., Garcés, M., Vergés, J., Haslam, I., Hardman, M., 2011. New constraints on the Messinian sealevel drawdown from 3D seismic data of the Ebro Margin, western Mediterranean. Basin Research, 23(2), 123-145. DOI: 10.1111/j.1365.2117.2010.00477.x

Van Couvering, J.A., Castradori, D., Cita, M.B., Hilgen, F.J., Rio, D., 2000. The base of the Zanclean Stage and of the Pliocene Series. Episodes, 23(3), 179-187.

Viseras, C., Soria, J.M., Fernández, J., 2004. Cuencas neógenas postorogénicas de la Cordillera Bética. In: Vera, J.A. (ed.). Geología de España. SGE–IGME, 576-581.

Young, J.R., Flores, J.A., Wei, W., 1994. A summary chart of Neogene nannofossil magnetobiostratigraphy. Journal of Nannoplankton Research, 16, 21-27.

Manuscript received January 2014;
revision accepted February 2015;
published Online July 2015.